Statistical Thermodynamics of Block Copolymer Adsorption. 3. Interaction between Adsorbed Layers of Block Copolymers

O. A. Evers, J. M. H. M. Scheutjens,* and G. J. Fleer

Department of Physical and Colloid Chemistry, Wageningen University, Dreijenplein 6, 6703 HB Wageningen, The Netherlands

Received January 4, 1991; Revised Manuscript Received April 30, 1991

ABSTRACT: Recently, we presented a self-consistent-field theory for the adsorption of block copolymers from a multicomponent mixture. In this paper the theory is applied to the interaction between two layers of adsorbed block copolymers. The free energy of interaction is derived for two types of equilibrium: (i) all molecules are free to diffuse out of the gap (full equilibrium), and (ii) the amount between the surfaces of some molecules is constant (restricted equilibrium). For diblock copolymers with one strongly adsorbing and one weakly adsorbing or nonadsorbing block we find repulsive interaction curves at full equilibrium because bridging is unfavorable. This is in contrast with homopolymers, which always give attraction in full equilibrium. If the total amount of diblock copolymer is kept constant, the interaction in a good solvent is always repulsive. With increasing amounts the repulsion becomes stronger. The onset of interaction is found at a surface separation that is approximately twice the hydrodynamic layer thickness. This separation depends highly on the length of both blocks. We show how the interaction curves at different block lengths can be scaled onto one master curve. In a poor solvent attraction is found at large separations due to osmotic forces. For ABA triblock copolymers with adsorbing A segments and nonadsorbing B segments in a solvent that is good for B, we find attraction at large separations due to bridging.

Introduction

Polymers are widely used to modify the surface of colloidal particles. The main goal is to stabilize or flocculate these particles.[1-4] Diblock copolymers, like nonadsorbing terminally attached chains, are found to form very extended adsorption layers.[5-15] The amount on the surface can be considerably higher than in the case of homopolymers consisting of the adsorbing segments. As a result of these extended layers, colloidal particles covered with block copolymers in solvents that are better than θ solvents for the nonadsorbing blocks experience a strong steric repulsion when they approach each other. Formation of polymer bridges of adsorbing blocks is prevented by steric hindrance due to the nonadsorbing blocks. Hence, block copolymers are very effective in stabilizing colloidal suspensions and they are therefore utilized in many industrial products such as paints, inks, lubricants, coatings, and blends.

Recently, force measurements between mica sheets bearing adsorbed diblock copolymer[7,9-14] and triblock copolymer[9,10] have been reported. In good solvents long-range repulsive forces are found. The onset of repulsion is detected at separations between the mica sheets of up to 10 times the unperturbed radius of gyration of the nonadsorbing block. In solvents that are worse than θ solvents for the nonadsorbing blocks, attraction between the surfaces occurs. The magnitude of the attraction between adsorbed diblock copolymer layers as compared to the corresponding homopolymer varies considerably between the various experiments. For PV2P/PS (60 000–60 000 molecular weight) block copolymers in cyclohexane at 21 °C, Hadziioannou et al.[7] found a magnitude of attraction that was 5–10 times weaker than for a corresponding PS homopolymer. For PEO/PS (20 000–250 000) block copolymers in a solution of heptane–toluene (2:1 v/v), Marra and Hair[14] found the same order of magnitude for the attraction as for PS (300 000) homopolymer.

In a previous paper[16,17] we introduced a self-consistent-(mean) field theory for the adsorption of block copolymers (between two plates) from a multicomponent mixture, as a generalization of the Scheutjens–Fleer theory.[18-20] The theory is based on a lattice model in which no a priori assumptions are made about the conformations of the molecules. The probabilities of the various possible conformations are derived by optimizing the partition functions, after which the segment density profile near the surface is obtained. We have shown[16,17] how the conformation probabilities can be expressed in the potentials of every segment in the copolymer molecule. In this paper we will apply the theory to the case of the interaction between two adsorbed layers of block copolymers. The theory will be shortly reviewed, the concepts of full equilibrium and restricted equilibrium are introduced, and equations for the free energy of interaction are obtained from equations derived in refs 16 and 17. A collection of numerical results on the interaction between layers of adsorbed diblock and triblock copolymers are presented for both types of equilibrium. Special attention is paid to the effect of the chain composition on the interaction.

Theory

Model. A lattice between two parallel plates is used in order to make the number of possible conformations of the various molecules finite. The lattice is divided into equidistant layers parallel to the surfaces (see Figure 1). The layers are numbered $z = 1, 2, ..., M$ and have L lattice sites each. Every lattice site has Z nearest neighbors, a fraction λ_0 of which is found in the same layer and a fraction λ_1 in each of the adjacent layers. For example, in a hexagonal lattice $\lambda_0 = 6/12$ and $\lambda_1 = 3/12$.

We will use the subscript i to denote a particular type of molecule. A polymer molecule of type i is represented as a chain of connected segments numbered $s = 1, 2, ..., r_i$. Since copolymers contain in general more than one type of segment it is necessary to distinguish the type, denoted by A, B, C, ..., of each segment s. The number of segments A in one molecule i is denoted as r_{Ai}; obviously, $\sum_A r_{Ai} = r_i$. We assume that every lattice site is occupied by a segment or a solvent molecule and that every type of segment in the mixture has the same volume.

A density gradient in the mixture between the two plates will be found as a result of spatial restrictions, of mutual

0024-9297/91/2224-5558$02.50/0

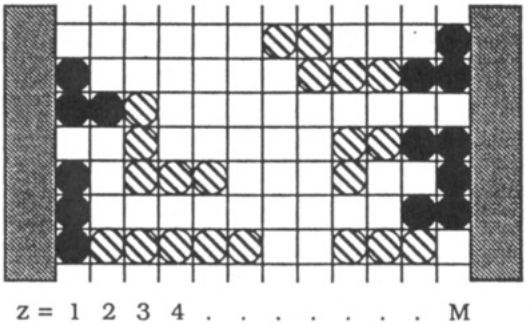

Figure 1. Three chains A_3B_5 and one chain $B_3A_5B_3$ in a lattice between two surfaces.

interactions between segments, and of interactions between segments and the surfaces. We use a mean-field approximation within each layer; i.e., we neglect density fluctuations parallel to the surfaces. In this approximation, only the distance to the surfaces is relevant. The volume fraction of molecules i in layer z is denoted by $\phi_i(z)$.

Apart from the mixture between the two surfaces, we introduce an infinitely large bulk solution as a reference. As shown in refs 16 and 17, it is not necessary that this bulk solution is in equilibrium with the mixture between the plates. The volume fraction of molecules i in the bulk solution is denoted by ϕ_i^b.

Segment Density Distribution. Every individual segment is subjected to a local potential, which depends on its physical nature and on the distance to the surfaces. We denote the local potential for a segment of type A in layer z as $u_A(z)$. In a previous paper[16,17] we derived an expression for $u_A(z)$ from the grand canonical partition function of the system. This potential can be subdivided into a part $u'(z)$, which only depends on z, and a part $u_A^{int}(z)$, which also depends on the type of segment:

$$u_A(z) = u'(z) + u_A^{int}(z) \tag{1}$$

The potentials are defined with respect to the infinitely large homogeneous bulk solution: $u_A^b = 0$. The "hard core" potential $u'(z)$ results from the fact that every segment has the same finite volume and is determined by the packing constraint $\sum_A \phi_A(z) = 1$. The potential $u_A^{int}(z)$ accounts for the energetic interactions of a segment of type A in layer z with neighboring segments or surface sites. We use the familiar Flory–Huggins interaction parameter χ_{AB} to account for the energetic interaction between A and B segments, and χ_{AS} for the interaction between A segments and surface sites. On average, a segment in layer z has $\langle\phi_B(z)\rangle Z$ contacts with B segments, where the contact fraction $\langle\phi_B(z)\rangle$ with B segments is given by

$$\langle\phi_B(z)\rangle = \lambda_1\phi_B(z-1) + \lambda_0\phi_B(z) + \lambda_1\phi_B(z+1) \tag{2}$$

We introduce a step-function profile for both adsorbents (surfaces), denoted as S and S′: $\phi_S(z)$ equals 1 for $z < 1$ and 0 for $z \geq 1$, and $\phi_{S'}(z)$ equals 1 for $z > M$ and 0 for $z \leq M$. Obviously, in the bulk solution $\phi_S^b = \phi_{S'}^b = 0$. The interaction potential $u_A^{int}(z)$ is given by

$$u_A^{int}(z) = \sum_B \chi_{AB}(\langle\phi_B(z)\rangle - \phi_B^b) \tag{3}$$

where S and S′ are also included in the summation over B. The summation on the right-hand side of eq 3 is to be taken over all segment types and surfaces if they are present in layers $z-1$, z, or $z+1$. The adsorption energy contribution to the sum is $\lambda_1\chi_{AS}$ for $z = 1$, $\lambda_1\chi_{AS'}$ for $z = M$, and zero for $1 < z < M$.

Let us first consider the case of monomer adsorption. For the segment density profile of monomers A in the mixture between the two plates in equilibrium with an infinite large bulk solution b we have the following Boltzmann equation:

$$\phi_A(z) = \phi_A^b \exp[-u_A(z)/kT] \tag{4}$$

This equation can be rewritten in terms of a segment weighting factor $G_A(z)$:

$$\phi_A(z) = \phi_A^b G_A(z) \tag{5}$$

where the segment weighting factor $G_A(z)$ is defined as

$$G_A(z) = \exp[-u_A(z)/kT] \tag{6}$$

For a chain molecule we have to take into account that the successive segments are connected to each other. First we introduce $G_i(z,s)$, the segment weighting factor of segment s in layer z. For example, if segment s is of type D, then $G_i(z,s)$ equals $G_D(z)$. The chain end distribution function $G_i(z,s|1)$ is defined as the average weighting factor of all possible conformations of a chain of s segments long starting at segment 1 anywhere in the lattice and ending with its last segment (s) in layer z. The analogous weighting factor for a chain starting at segment r_i anywhere in the lattice and ending at segment s in layer z is denoted as $G_i(z,s|r_i)$. In order to obtain the volume fraction $\phi_i(z,s)$ of segment s of molecules i in layer z we should multiply the weighting factors of the two chain parts, $G_i(z,s|1)$ and $G_i(z,s|r_i)$, respectively. However, we have to correct for double counting of the segment weighting factor $G_i(z,s)$ of segment s (which is in layer z), since this weighting factor is contained in both chain end distribution functions:

$$\phi_i(z,s) = C_i G_i(z,s|1)G_i(z,s|r_i)/G_i(z,s) \tag{7}$$

where C_i is a normalization constant depending on the type of molecule and which will be derived below. The chain end distribution functions $G_i(z,s|1)$ and $G_i(z,s|r_i)$ are found from a recurrence relation. Obviously, $G_i(z,1|1) = G_i(z,1)$ and $G_i(z,r_i|r_i) = G_i(z,r_i)$. If segment s finds itself in layer z, then the connected segment $s-1$ should be located in one of the layers $z-1$, z, or $z+1$. Thus, we can divide the chain end distribution function $G_i(z,s|1)$ into two factors:

$$G_i(z,s|1) = G_i(z,s)\langle G_i(z,s-1|1)\rangle \tag{8}$$

where $\langle G_i(z,s-1|1)\rangle$ is the neighbor average of $G_i(z,s-1|1)$, defined in the same way as $\langle\phi_B(z)\rangle$ in eq 2. In fact, eq 8 is a recurrence relation, valid for $s > 1$. For $G_i(z,s|r_i)$ we have a similar recurrence relation:

$$G_i(z,s|r_i) = G_i(z,s)\langle G_i(z,s+1|r_i)\rangle \tag{9}$$

The volume fraction profile $\phi_i(z)$ of all segments of molecules i in layer z is simply given by the summation of $\phi_i(z,s)$ over all r_i segments:

$$\phi_i(z) = \sum_{s=1}^{r_i} \phi_i(z,s) \tag{10}$$

If we want to calculate the volume fraction of, for instance, only the A segments of molecules i, $\phi_{Ai}(z)$, we perform the summation of $\phi_i(z,s)$ only over those segments s that are of type A.

Full Equilibrium and Restricted Equilibrium. In the preceding section we discussed briefly how the density profiles of the various segment types present in the mixture between the two plates are calculated from the segment

potential profiles. To that end, the normalization constant C_i has to be found from the boundary conditions. We distinguish two cases: full equilibrium and restricted equilibrium.

In full equilibrium all molecules are free to diffuse in and out of the gap between the two plates and all molecule types are in equilibrium with an (infinitely large) bulk solution of constant composition. When the plates are brought closer, the chemical potential μ_j of each component j remains constant and equal to that in the bulk solution. As a generalization of the Flory–Huggins equation, we derived in Appendix I of ref 17

$$(\mu_j - \mu_j^*)/kT = \ln \phi_j^b + 1 - r_j \sum_l \phi_l^b/r_l - \frac{r_j}{2}\sum_{A,B}(\phi_A^b - \phi_{Aj}^*)\chi_{AB}(\phi_B^b - \phi_{Bj}^*) \quad (11)$$

where the superscript * refers to the reference state of pure amorphous components, and $\phi_{Aj}^* = r_{Aj}/r_j$ is the volume fraction of A segments in pure amorphous j.

In the equilibrium bulk solution, the potentials u_A^b and u'^b are zero by definition. Then it follows from applying eq 7 to this bulk solution that the normalization constant C_j is given by

$$r_j C_j = \phi_j^b \quad (12)$$

Hence, in full equilibrium C_j is a constant that does not depend on the plate separation M.

In restricted equilibrium some components (denoted by the subscript j) are free to diffuse from the gap to the bulk solution (the "mobile" components), while others (the "restricted" components, indicated by the subscript k) have no time to establish equilibrium with the bulk solution. This situation may occur if the time scale of the variation in the plate distance (e.g., during a Brownian collision) is much shorter than the time necessary for the transfer of the molecules (e.g., long chains with a small diffusion constant). For the mobile components, μ_j and C_j are constant and given by eqs 11 and 12, respectively. For the restricted components, the contact with the bulk solution is lost if the plates come close and μ_k and C_k become a function of the plate separation M. A reasonable model is to assume that for these components the total amount of polymer θ_k is constant (i.e., the independent of M). The latter quantity is defined as

$$\theta_i = \sum_z \phi_i(z) \quad (13)$$

and gives the number of equivalent monolayers of each component between the plates. The total number of chains or end segments $s = r_i$ (per surface site of one plane) is θ_i/r_i. From eq 7, with $s = r_i$, we find $\phi_i(z,r_i) = C_i G_i(z,r_i|1)$. Summing over z gives $\sum_z \phi_i(z,r_i) = \theta_i/r_i$, or

$$r_i C_i = \theta_i / G_i(r_i|1) \quad (14)$$

where the chain weighting factor $G_i(r_i|1)$ is defined as

$$G_i(r_i|1) = \sum_z G_i(z,r_i|1) = \sum_z G_i(z,1|r_i) \quad (15)$$

Equation 14 is general and applies to both the mobile (j) and the restricted (k) components. For the mobile components, θ_j and $G_j(r_j|1)$ change in the same ratio, making C_j constant and independent of M; in this case eq 12 is still valid. For the restricted components θ_k is constant, and C_k becomes a function of M since $G_k(r_k|1)$ varies with M.

For the restricted components, μ_k varies with M and eq 11 no longer applies. However, μ_k can be computed directly from C_k through the following relation:[16,17]

$$(\mu_i - \mu_i^*)/kT = \ln (r_i C_i) + 1 - r_i \sum_l \phi_l^b/r_l - \frac{r_i}{2}\sum_{A,B}(\phi_A^b - \phi_{Ai}^*)\chi_{AB}(\phi_B^b - \phi_{Bi}^*) \quad (16)$$

This relation is again valid for both the mobile (j) and restricted (k) components. In the former case, where both μ_j and C_j are independent of M, eq 16 reduces to eq 11. For the latter, $C_k(M)$ is computed from eq 14 and $\mu_k(M)$ from eq 16.

Note that the use of eq 14 implies $u_A^b = u'^b = 0$ in the bulk solution, also for segments occurring only in restricted components. For these components, the bulk solution may be chosen arbitrarily; however, the most convenient choice is the composition of the solution at large plate separations, when full equilibrium applies.

Free Energy of Interaction. At plate separation M the number of molecules of each type i in the gap is $L\theta_i(M)/r_i$. With varying M the amount θ_k for the restricted components is constant, whereas $\theta_j(M)$ for the mobile components changes by an amount $\Delta\theta_j$: $L\Delta\theta_j(M)/r_j$ molecules of each mobile component are transferred to the bulk solution. The free energy changes by an amount $\Delta A - L\sum_j \mu_j \Delta\theta_j/r_j$, where ΔA is the free energy difference due to the molecules in the gap, and the second term corresponds to the free energy of transfer of the mobile components. If we define an excess free energy A^{ex} as

$$A^{ex}(M) = A(M) - L\sum_j \theta_j(M)\mu_j/r_j \quad (17)$$

we can write for the free energy of interaction A^{int}

$$A^{int}(M) = A^{ex}(M) - A^{ex}(\infty) \quad (18)$$

Both terms of the right-hand side of eq 17 tend to infinity as $M \to \infty$, but $A^{ex}(M)$ is finite and well-defined, with $dA^{ex}/dM \to 0$ as $M \to \infty$. Note that A^{ex} may not be identified with the Gibbs excess free energy A^σ, which should be defined as $A^\sigma(M) = A(M) - LM\sum_i \phi_i^b \mu_i/r_i$, where the summation extends over all components.

The free energy $A(M)$ of the system between the plates follows from the partition function. In our previous paper[16,17] we derived the following expression:

$$\frac{A(M) - A^*}{LkT} = -\sum_i \frac{\theta_i^{ex}}{r_i} - \sum_z \frac{u'(z)}{kT} - \frac{1}{2}\sum_{z,A',B'} \chi_{A'B'}(\phi_{A'}(z) \times \langle \phi_{B'}(z) \rangle - \phi_{A'}^b \phi_{B'}^b) + \sum_i \frac{\theta_i(\mu_i - \mu_i^*)}{r_i kT} \quad (19)$$

where $\theta_i^{ex} = \theta_i - M\phi_i^b$ is defined as

$$\theta_i^{ex} = \sum_z \{\phi_i(z) - \phi_i^b\} \quad (20)$$

The summation over i in eq 19 includes all molecule types present between the plates and in the bulk solution, both the mobile (j) and restricted (k) components. The primes attached to A′ and B′ indicate that the surfaces S and S′ are not included in the double summation (unlike eq 3, where the surfaces have to be accounted for). The bulk solution concentrations in eqs 19 and 20 are those corresponding to $u'^b = 0$; for the restricted components the choice is arbitrary, but as stated above the equilibrium composition at $M \to \infty$ is most convenient.

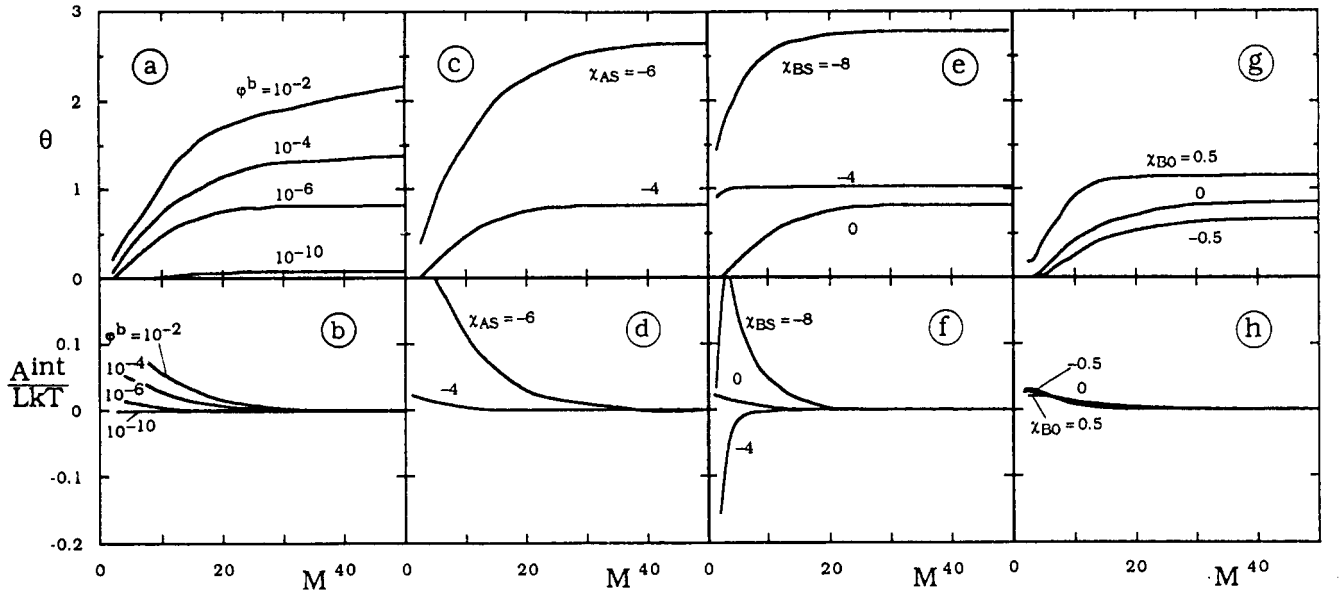

Figure 2. Amount of polymer between the plates (top diagrams) and interaction curves (bottom diagrams) of an $A_{50}B_{100}$ diblock copolymer at full equilibrium. In each diagram the curve for $\chi_{AS} = -4$ (adsorbing A segments), $\chi_{BS} = 0$ (nonadsorbing B segments), all the other χ parameters zero, and $\phi^b = 10^{-6}$ is given as reference and one of these parameters is varied (their values are indicated). Thus, the effect of the solution concentration is shown in (a) and (b), that of χ_{AS} in (c) and (d), and that of χ_{BS} in (e) and (f). Finally, the effect of the solvent quality for the B segments is given in (g) and (h).

(a) Full Equilibrium. In full equilibrium all components are mobile ($i = j$, $\theta_k = 0$). Upon substitution of eq 19 into eq 17 the terms $\theta_i(\mu_i - \mu_i^*)$ cancel:

$$\frac{A^{ex}(M)}{LkT} = -\sum_i \frac{\theta_i^{ex}}{r_i} - \sum_z \frac{u'(z)}{kT} - \frac{1}{2}\sum_{z,A',B'} \chi_{A'B'}(\phi_{A'}(z) \times \langle\phi_{B'}(z)\rangle - \phi_{A'}^b\phi_{B'}^b) \quad (21)$$

(b) Restricted Equilibrium. Now we have to distinguish between the mobile components j and the restricted components k. In eq 17 plus 19 only the terms $\theta_j(\mu_j - \mu_j^*)$ cancel:

$$\frac{A^{ex}(M)}{LkT} = -\sum_i \frac{\theta_i^{ex}}{r_i} - \sum_z \frac{u'(z)}{kT} - \frac{1}{2}\sum_{z,A',B'} \chi_{A'B'}(\phi_{A'}(z)\langle\phi_{B'}(z)\rangle - \phi_{A'}^b\phi_{B'}^b) + \sum_k \frac{\theta_k(\mu_k - \mu_k^*)}{r_k kT} \quad (22)$$

The summation over i includes all components, that over k only the restricted ones. The chemical potentials $\mu_k - \mu_k^*$ are found from eqs 16 and 14.

Computational Aspects. We have related the segment densities $\phi_A(z)$ to the segment potentials $u_A(z)$ in a self-consistent way. From an initial guess for the segment potential profiles $u_A(z)$ the corresponding segment density profiles $\phi_A(z)$ are calculated with eqs 6, 7, and 10. To calculate the normalization constant C_i necessary in eq 7 we use eq 11 or 16, depending on whether the molecules are free to diffuse out of the gap between the two plates or not. The values obtained for $\phi_A(z)$ are checked on the M boundary conditions $\sum_A \phi_A(z) = 1$, and in combination with an initial guess for the M hard core potentials $u'(z)$ the initial guess for the segment potentials is checked on its consistency with the $\phi_A(z)$ values, using eqs 1 and 3.

In references 16 and 17 we presented an implicit set of simultaneous equations from which the equilibrium values of $u_A(z)$ and $u'(z)$ are calculated by standard numerical techniques.

Results

In this section we present numerical results for some typical cases of interaction between adsorbed layers of copolymers for a hexagonal lattice ($\lambda_0 = 6/12$). The effect of chain composition on the free energy of interaction will be discussed in relation to the effect of parameters such as solvent quality and surface affinity. Both full and restricted equilibrium will be considered. In this paper, we will deal with two-component mixtures only, viz., a copolymer in a monomeric solvent.

Full Equilibrium. For adsorbing homopolymers in full equilibrium with a bulk solution, the interaction between two plates has been found to be always attractive.[20] With decreasing plate separation desorption of the homopolymer occurs in order to maintain equilibrium between the mixture in the gap and the bulk solution, eventually resulting in one monolayer of polymer segments and solvent monomers in contact with both surfaces. The attractive force between the adsorbed layers of homopolymer at full equilibrium is due to bridging; i.e., chains are simultaneously adsorbed on both surfaces. At the smallest separation of one monolayer between the plates, all polymer segments are bridging segments. Because of this bridging, desorption is not complete.

As we have shown in an earlier publication,[16,17] diblock copolymers adsorb with the adsorbing block in a relatively flat conformation close to the surface and the more weakly (or non-) adsorbing block in one dangling tail. These copolymers are not likely to form bridges. When formation of bridges is negligible, repulsive forces are likely to be found even in full equilibrium. Therefore, with decreasing plate separation we expect these copolymers to desorb more strongly than homopolymers.

In Figure 2 the total amount θ of diblock copolymer between the two plates (top diagrams) and the free energy of interaction A^{int} (bottom diagrams) are given as a function of the plate separation M, for an $A_{50}B_{100}$ diblock copolymer under various conditions. Unless indicated otherwise, the A segments are adsorbing ($\chi_{AS} = -4$) and the B segments nonadsorbing ($\chi_{BS} = \chi_{OS} = 0$). All other χ parameters are zero, and $\phi^b = 10^{-6}$. Under most conditions the interaction

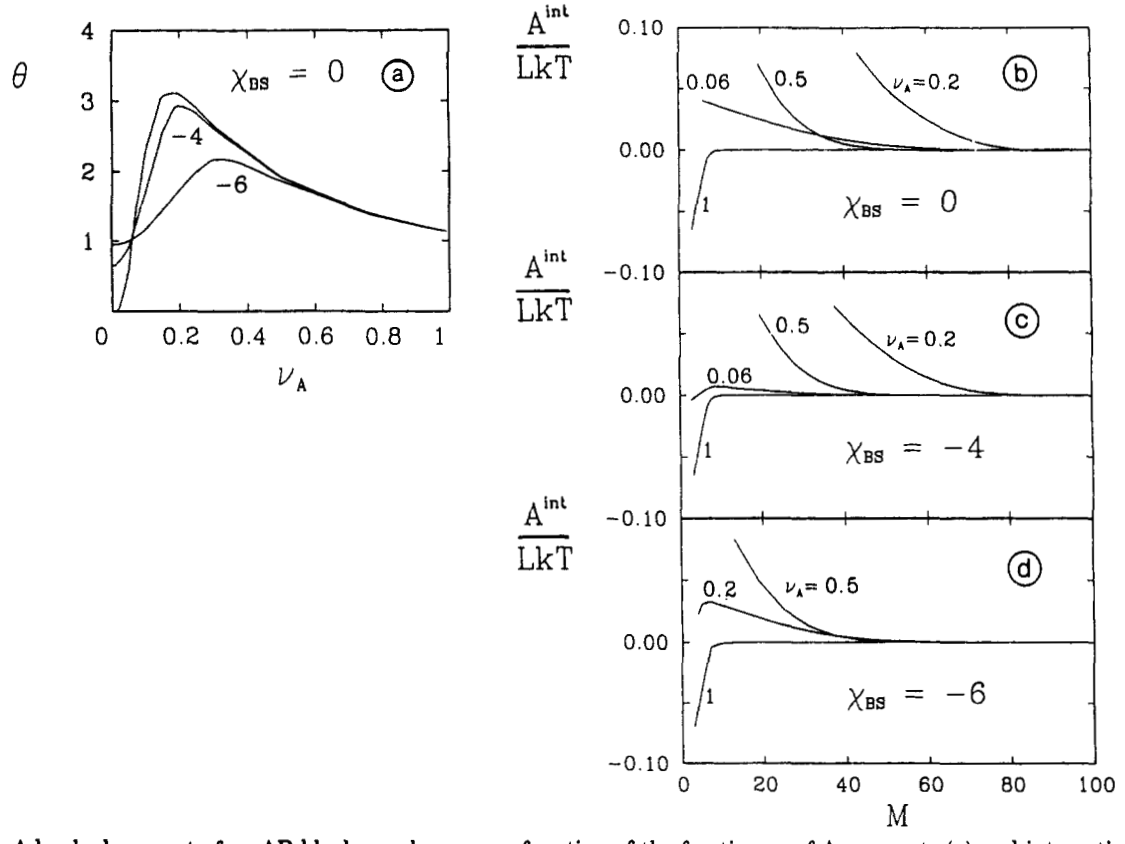

Figure 3. Adsorbed amount of an AB block copolymer as a function of the fraction ν_A of A segments (a) and interaction curves at full equilibrium (b–d) for different values of ν_A, at three surface affinities of the more weakly (or non-) adsorbing B block. The A segments are strongly adsorbing ($\chi_{AS} = -8$). Other parameters: $\chi_{AO} = \chi_{AB} = \chi_{BO} = 0$, $r_A + r_B = 250$, and $\phi^b = 10^{-4}$.

between the plates is found to be repulsive. When the total amount of diblock copolymer (which in this case is nearly equal to the adsorbed amount) is increased, the interaction becomes more repulsive because a higher amount of copolymer at the same plate separation results in a stronger steric hindrance between the nonadsorbing blocks. Increasing the total amount θ can be achieved by an increase of ϕ^b, an increase of χ_{BO}, or a decrease of χ_{AS}.

Interaction curves for four different solution concentrations ϕ^b are shown in diagram b. In all cases the interaction between the adsorbed layers is repulsive, the more so as ϕ^b increases. We will discuss the onset of interaction in connection with Figures 2h and 3. In parts c and d the effect of surface affinity of the adsorbing A segments is shown. As the surface affinity increases, i.e., with decreasing χ_{AS}, the total amount increases, as can be expected since a higher surface affinity gives a better compensation of the loss of entropy when a copolymer molecule adsorbs. As a result of the higher adsorbed amounts the interaction becomes more repulsive when χ_{AS} decreases.

The effect of the surface affinity of the B segments is displayed in parts e and f. The A segments are adsorbing ($\chi_{AS} = -4$). For $\chi_{BS} = 0$ the interaction is repulsive as in parts b and d. The interaction curve for $\chi_{BS} = -4$ is found to be attractive and represents in fact a homopolymer of 150 segments since χ_{AS} is also −4 and all other χ parameters are zero. The weak maximum in θ in this case has been discussed by Scheutjens and Fleer[20] and is due to the contribution of bridging chains to θ in addition to the chains adsorbing on one of the plates only. The total amount θ of homopolymer ($\chi_{AS} = \chi_{BS} = -4$) is higher than that of block copolymers with $\chi_{AS} = -4$ and $\chi_{BS} = 0$. In this case the block copolymer is more weakly adsorbed than the homopolymer. However, diblock copolymers of the same length as a homopolymer can achieve a much higher adsorbed amount if the chains are sufficiently strongly anchored, because of the dangling B block. We have shown this effect in a previous paper.[21] Such a situation occurs for $\chi_{BS} = -8$, where the A block becomes the weakly adsorbing block. At relatively large plate separation the interaction is strongly repulsive, but around $M = 4$ it passes a maximum. At still smaller plate separation the energy of interaction decreases due to bridge formation by the strongly adsorbing B blocks, but it remains weakly repulsive at $M = 2$. Bridging is entropically favorable since the number of conformations with many adsorbed segments increases considerably when the chain can adsorb on two opposing surfaces at the same time. Essentially, in this case two thin layers of adsorbed B blocks mix and form a thicker layer in which the B blocks cross the gap several times. Attraction occurs only if the more weakly adsorbing blocks are not too long.

Not only the adsorption energy, but also the solvent quality affects the adsorption and interaction curves. Diagrams g and h show the effect of varying the solvent quality χ_{BO} for the nonadsorbing B block. When the solvent quality becomes poor ($\chi_{BO} > 0$), the dangling B blocks assume a more collapsed conformation and, hence, the thickness of the adsorbed layer decreases. Therefore the onset of interaction decreases with increasing χ_{BO} (although this can hardly be seen on the scale used in Figure 2h). Because the adsorbed amount of copolymer is higher for poorer solvents, the interaction between the plates at small M becomes more repulsive when the solvent quality decreases (increasing χ_{BO}). Hence, the repulsion curves in Figure 2h intersect each other.

The adsorbed amount and the free energy of interaction of an AB diblock for different adsorption energies of the B segments are shown in Figure 3 as a function of the

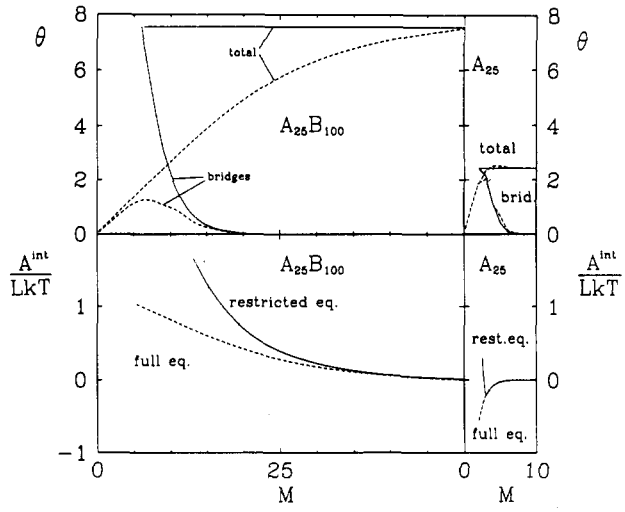

Figure 4. Comparison between adsorption and interaction curves at full equilibrium (dashed curves) and restricted equilibrium (full curves) of an $A_{25}B_{100}$ diblock copolymer (left-hand side) and an A_{25} homopolymer (right-hand side). The total amounts of polymer at large surface separation correspond to equilibrium adsorption at $\phi^b = 10^{-4}$. The A segments are strongly adsorbing ($\chi_{AS} = -10$) and the B segments do not adsorb ($\chi_{BS} = 0$). Other parameters: $\chi_{AO} = \chi_{AB} = 0.5$, $\chi_{BO} = 0$.

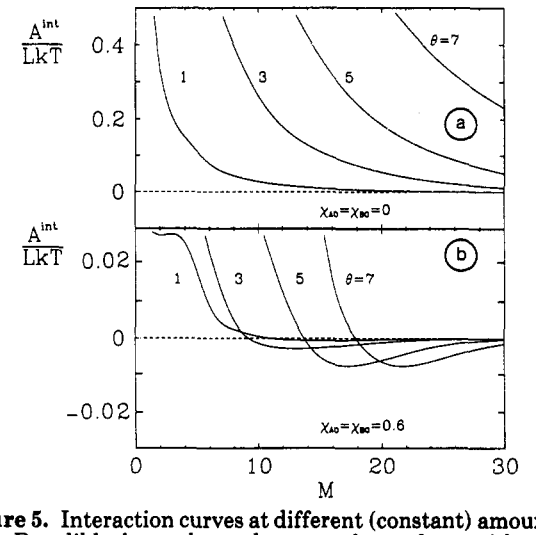

Figure 5. Interaction curves at different (constant) amounts of an $A_{50}B_{100}$ diblock copolymer between the surfaces with a good solvent (a) and a poor solvent (b) for the A and B segments. Parameters: $\chi_{AS} = -10$, $\chi_{BS} = 0$, $\chi_{AB} = 0$.

chain composition. The diblock copolymer is 250 segments long with $\phi^b = 10^{-4}$, the A segments are strongly adsorbing ($\chi_{AS} = -8$), χ_{BS} is 0, −4, or −6, and all other χ parameters are zero. In diagram a the adsorbed amount θ^a is shown as a function of the fraction ν_A of A segments per chain, at three different values of χ_{BS}. A maximum in the adsorbed amount is observed. As already explained in a previous paper,[21] at low ν_A the attachment is too weak. With increasing ν_A, the leveling off toward the maximum is due to saturation of the surface with A segments, and the decrease beyond the maximum occurs because, at full surface saturation, the length of the nonadsorbed B tails decreases. Since the interaction between the adsorbed layers depends highly on the adsorbed amount, we expect a strong effect of the composition of the copolymer on the free energy of interaction. This is indeed the case, as can be seen in diagrams b–d. Interaction curves for four (a and b) or three (d) different values of ν_A are shown. The strongest repulsion is found for those values of ν_A that correspond to the highest adsorbed amount. Thus, for χ_{BS} equal to zero or −4 we find the strongest repulsion for $\nu_A = 0.2$, whereas for $\chi_{BS} = -6$ the repulsion is stronger for $\nu_A = 0.5$ than that for $\nu_A = 0.2$. In this latter case, the strongest repulsion occurs for ν_A around 0.35 (not shown). With increasing length of the B block (i.e., decreasing ν_A) and sufficient adsorption affinity, the adsorbed layer becomes thicker and therefore the onset of interaction will be found at larger plate separations.

Restricted Equilibrium. When the polymer is unable to diffuse out of the gap between the two plates, the mixture is in a restricted equilibrium. In this case the total amount θ of polymer is constant when the surfaces are brought closer, and the chemical potential of the polymer varies with plate separation. The free energy of interaction is zero at large plate separation and infinite when $M < \theta$ (the segments are incompressible).

The difference between a block copolymer $A_{25}B_{100}$ (with $\chi_{BS} = 0$) and the corresponding homopolymer A_{25} is shown in Figure 4, both for the adsorbed amount (top) and for the interaction curves (bottom), in full equilibrium and in restricted equilibrium. The A segments are strongly adsorbing ($\chi_{AS} = -10$), and the solvent quality is good for the B segments ($\chi_{BO} = 0$) and poor for the A segments ($\chi_{AO} = \chi_{AB} = 0.5$). The equilibrium volume fraction ϕ^b is 10^{-4}, which corresponds for the $A_{25}B_{100}$ copolymer with an equilibrium adsorption at large plate separation of $\theta = 7.6$ and for the A_{25} homopolymer to $\theta = 2.4$. To obtain the same reference free energy in the case of restricted equilibrium we used $\theta = 7.6$ for the diblock copolymer and $\theta = 2.4$ for the homopolymer. Since the solvent quality is poor for the A segments, a maximum in θ is found for the A_{25} homopolymer in full equilibrium, as a result of additional adsorption due to bridging at the onset of the interaction. The homopolymer in full equilibrium gives only attraction, whereas in restricted equilibrium an attractive minimum is observed because of bridging. For the diblock copolymer repulsive interaction curves are obtained, both in full and restricted equilibrium, as a result of the steric repulsion between the nonadsorbing B blocks. The repulsion is stronger in restricted equilibrium since the copolymers cannot leave the gap between the plates. In full equilibrium, the fraction of bridging molecules in the case of the $A_{25}B_{100}$ diblock copolymer is much lower (by a factor of 10) as compared to the A_{25} homopolymer. The steric hindrance caused by the B blocks strongly reduces the possibility of bridging by the adsorbing A segments. In restricted equilibrium, where the chains are forced to bridge when the plates are brought closer together, the copolymer chains that are in contact with both surfaces do not give rise to attraction because of the loss of entropy of the B blocks.

Figure 5 shows interaction curves for an $A_{50}B_{100}$ diblock copolymer in restricted equilibrium at different (constant) amounts θ, for two (equal) solvent qualities for the A and B segments. The A segments are strongly adsorbing ($\chi_{AS} = -10$, $\chi_{BS} = 0$). If the solvent quality is good for the A and B segments (Figure 5a) we find only repulsion. As the amount of copolymer increases, the interaction becomes more repulsive because of the higher density and, consequently, increasing steric hindrance between the copolymer layers. At a very poor solvent quality ($\chi = 0.6$) for the A and B segments (Figure 5b), the interaction curves have an attractive minimum at large plate separations. The reason for this attractive minimum is not bridging but osmotic attraction in the bad solvent, which causes the surface to act as a nucleus for phase separation. In other words, osmotic attraction occurs since in this case the osmotic pressure decreases when polymer chains overlap. This effect is shown in more detail in Figure 6.

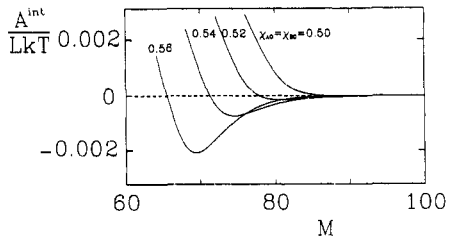

Figure 6. Effect of the solvent quality for the A and B segments on the interaction curves of an $A_{15}B_{200}$ diblock copolymer at constant amount of polymer (θ = 21.5). Parameters: χ_{AS} = −20, χ_{BS} = 0, χ_{AB} = 0.

In Figure 6, interaction curves of an $A_{15}B_{200}$ diblock copolymer in restricted equilibrium (θ = 21.5) are given, for various (equal) solvent qualities for the A and B segments. The A segments adsorb strongly (χ_{AS} = −20) and the B segments do not adsorb (χ_{BS} = 0). An attractive minimum occurs when the solvent quality for the A and B segments becomes greater than 0.5. Hence, the phase separation behavior of strongly adsorbed diblock copolymers is similar to that of infinitely long chains in solution, for which the critical χ value for phase separation equals 0.5. This can be expected since adsorbed diblock copolymers, like anchored chains,[22,23] have essentially no translational entropy. At weaker adsorption, a slightly higher χ value is necessary for attraction to occur (not shown).

In comparison with grafted chains,[22,23] the interaction curves are almost quantitatively the same if the amount and length of the nonadsorbing blocks are the same as those of the grafted polymer. The only difference is that the curves for adsorbed diblock copolymers are shifted a few lattice layers toward higher plate separations since the joints between the A and B blocks of the adsorbed copolymer are, on average, further from the surface than the anchoring points of the grafted polymer. Indeed, adsorbed diblock copolymers are often modeled as grafted chains. For example, Whitmore and Noolandi, applying their self-consistent-field theory to study the properties of adsorbed block copolymers, assumed that the adsorbing blocks are constrained within a thin layer at the surface.[24] The curves given in Figure 6 agree well with their results.

Next we consider the influence of the chain composition of block copolymers on the interaction. Interaction curves of an $A_{100}B_n$ diblock copolymer and a $B_{n/2}A_{100}B_{n/2}$ triblock copolymer with an A block of 100 segments and varying length of the B block(s) are shown in Figure 7, for the case of restricted equilibrium. As before, the A segments adsorb strongly (χ_{AS} = −10) and the B segments have no affinity for the surface (χ_{BS} = 0). The solvent quality is good for the B segments (χ_{BO} = 0) and poor for the A segments (χ_{AO} = 0.5). The equilibrium adsorbed amounts at large plate separations are calculated at a fixed solution volume fraction of 10^{-4}. Since the solvent quality is good for the nonadsorbing block we obtain, as discussed before, only repulsive interaction curves. Parts a and b of Figure 7 give results for the diblock copolymer, parts c and d for the triblock copolymer. Figure 7e shows the hydrodynamic layer thickness of the adsorbed block copolymers, calculated with the method of Scheutjens et al.[25] The permeability constant c_h of the polymer is taken as 1. The thickness increases virtually linearly with the length of the nonadsorbing B block. Hence, the plate separation at which the adsorbed layers overlap, i.e., the onset of interaction, will increase with increasing length of the B block. If we assume the onset of interaction to

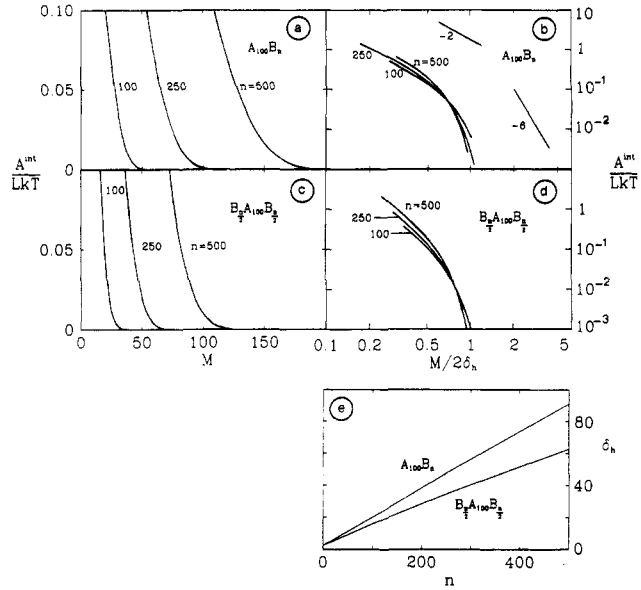

Figure 7. Effect of the length of the nonadsorbing B block on the interaction curves at restricted equilibrium of $A_{100}B_n$ diblock copolymers (a,b) and $B_{n/2}A_{100}B_{n/2}$ triblock copolymers (c,d). The A block contains 100 strongly adsorbing A segments (χ_{AS} = −10). The total amounts correspond to an equilibrium adsorption at large plate separation from a bulk solution with $\phi^b = 10^{-4}$. The dependence of the hydrodynamic layer thickness of the adsorbed layer at large plate separation is shown in (e). Parameters: χ_{BS} = 0, χ_{AO} = 0.5, χ_{AB} = χ_{BO} = 0.

be located at twice the hydrodynamic layer thickness δ_h, we might expect the curves to merge into one master curve if A^{int} is plotted versus $M/2\delta_h$. In order to show this, we replotted the data of Figure 7a and c, respectively, with logarithmic scales in Figure 7b and d. The curves nearly merge into one master curve. At plate separations below δ_h ($M/2\delta_h < 0.5$), the free energy of interaction A^{int} for the diblock copolymer scales approximately as $(M/2\delta_h)^{-2}$. At larger plate separations, where the adsorbed layers just overlap, we do not find a simple scaling relation between A^{int} and $M/2\delta_h$, but the dependence is then much stronger.

For the BAB triblock copolymer, the onset of interaction is found at much smaller plate separations as compared to the AB diblock copolymer (Figure 7c). The hydrodynamic layer thickness (Figure 7e) is also much lower for the BAB triblock copolymer. The main reason is that the B blocks of the triblock copolymer are shorter. Moreover, we have shown in an earlier publication[16,21] that the number of adsorbed chains of a BAB triblock copolymer is lower than that of the corresponding AB diblock copolymer, provided the (total) number of B segments per chain is the same. (Note that in Figure 10b of ref 21 the curve for $B_{m/2}A_{100}B_{m/2}$ was erroneously labeled as $B_mA_{100}B_m$.) However, if compared with $A_{100}B_n$ molecules, of which the lengths of the B blocks are the same, the onset of interaction is at a larger separation (Figure 7c) since the adsorbed layer is denser and hence the tails of the BAB triblock copolymer are more strongly stretched. As in the case of the AB diblock copolymer, the interaction curves for the triblock copolymer nearly merge into one master curve. The slope is higher for triblocks because of the denser adsorbed layer.

Figure 8 shows the effect of varying the length of the adsorbing A block on the adsorbed amount, on the hydrodynamic layer thickness, and on the interaction between layers of adsorbed AB diblock copolymer in restricted equilibrium. The interaction parameters are the same as in Figure 7, the length of the nonadsorbing B block is 250. The equilibrium adsorbed amount at large

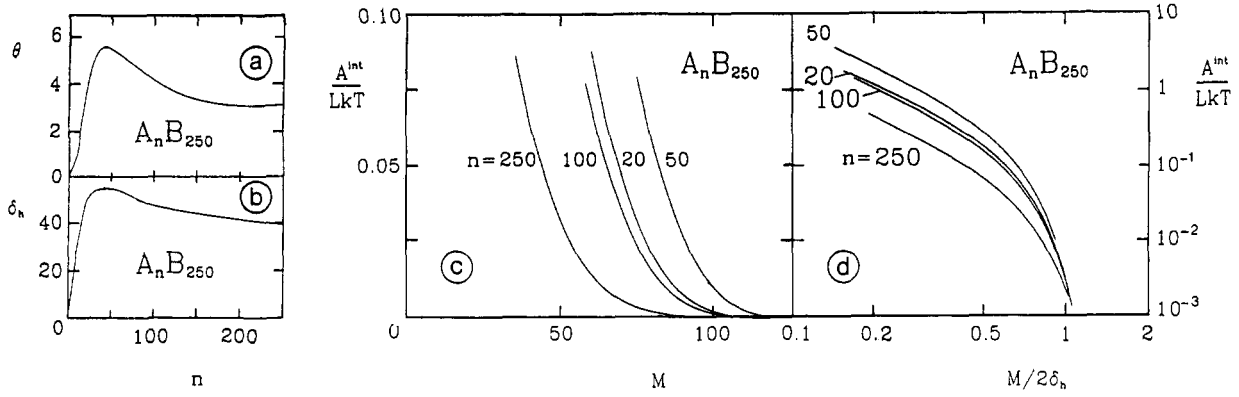

Figure 8. Equilibrium adsorbed amount (a) and hydrodynamic layer thickness (b) as a function of the length of the adsorbing A block ($\chi_{AS} = -10$) of an A_nB_{250} diblock copolymer having nonadsorbing B segments ($\chi_{BS} = 0$). In (c) interaction curves are given for four different lengths n of the A block. In (d) the curves of (c) are scaled with δ_h and replotted with logarithmic scales. The total amount (which is virtually equal to the adsorbed amount) corresponds to an equilibrium adsorption at $\phi^b = 10^{-4}$. The permeability constant c_h is 1. Parameters: $\chi_{AO} = 0.5$, $\chi_{AB} = \chi_{BO} = 0$.

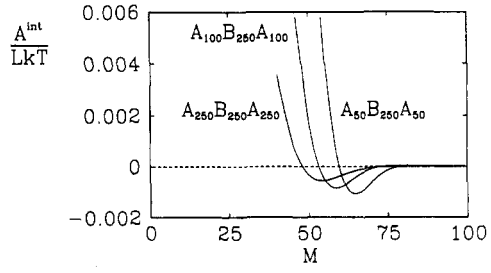

Figure 9. Interaction curves of an $A_nB_{250}A_n$ triblock copolymer having a nonadsorbing B block of 250 B segments ($\chi_{BS} = 0$) and varying length n of the adsorbing A block ($\chi_{AS} = -10$). The total amounts of polymer correspond to an equilibrium adsorption at large surface separation when $\phi^b = 10^{-4}$. Parameters: $\chi_{AO} = 0.5$, $\chi_{AB} = \chi_{BO} = 0$.

plate separation shows a maximum as a function of n (Figure 8a), for the same reason as in Figure 3a. The value of n corresponding to this maximum will be referred to as the "optimal A block length". The hydrodynamic layer thickness follows closely the adsorbed amount, as can be seen in Figure 8b. In Figure 8c interaction curves are given for four values of n. For $n = 50$ we find the most repulsive interaction curve and the largest interaction range. This is easily understood since a block length of 50 A segments is close to the optimal A block length (Figure 8a). In Figure 8d we have replotted the data of Figure 8c with logarithmic scales as in Figure 7b,d. We note that for n values up to 100 and for $M/2\delta_h$ near 1 the curves nearly merge into one master curve. The top curve is for the optimal A block length, $n = 50$. For all curves a slope of −2 is found when $M < \delta_h$. For larger values of M the slope decreases far more steeply.

In Figure 9 interaction curves are shown for an $A_nB_{250}A_n$ triblock copolymer at various lengths n of the adsorbing A blocks under the same conditions as in Figure 7. Again, the length of the nonadsorbing B block is kept constant at 250 segments. Because these triblock copolymers have adsorbing blocks at both sides of the molecule, they are able to form bridges. Therefore, the curves show an attractive minimum at large plate separations. The largest onset of interaction and the deepest attractive minimum is found for an A block length of 50 segments because this block length is close to the optimal A block length of this triblock copolymer (not shown).

Discussion

We have shown how the free energy of interaction can be calculated from our self-consistent-field theory[16,17] for full and restricted equilibrium. The case of restricted equilibrium is physically the most relevant, since in practice the time scale in which surfaces are brought closer is much shorter than that of the transfer of chains. Therefore we will compare our predictions for diblock copolymers in restricted equilibrium with experimental results.

Force–distance profiles for two cylindrical mica sheets covered with polymer can be measured directly with the surface force apparatus.[26-28] Several authors[7,9-14] have reported results on the interaction between adsorbed diblock copolymer layers obtained with this apparatus. The normalized force F/R, where R is radius of the mica cylinders, is measured typically up to 10 mN/m. Using the Deryagin approximation,[29] the measured force F/R between the two crossed cylinders can be related to the free energy of interaction for two planar surfaces as calculated with our theory:

$$A^{int}/L = Fa_s/2\pi R \qquad (23)$$

where a_s is the cross-sectional area of a lattice site. If we assume a segment to have a cross-sectional area of 0.06 nm^2, then the upper experimental limit of 10 mN/m would correspond to a free energy of interaction of 0.024 kT per surface site.

In agreement with the experimental results of Patel et al.[7,9,10] and Ansarifar and Luckham,[12,13] we do not find, in the range $A^{int}/LkT < 0.024$, a clear power law of the type $A^{int} \sim D^x$, where D is the distance between the plates. At large plate separations, the exponent x as obtained from Figures 7b and 8d varies between −4 and −6. These values are consistent with the experimental results of Patel et al. and Ansarifar and Luckham, who found exponents of approximately −4. As in practice polydispersity softens the hairy layer, the experimental exponent may be smaller than the prediction for homodisperse tails. At very high compression, the exponent is much smaller: $A^{int} \sim D^{-9/4}$ as estimated from scaling principles for terminally attached chains.[30] From the results of our theory it follows that an exponent of −2 would be found at smaller separations than reached in the experiments.

The effect of the chain length of the nonadsorbing block of a diblock copolymer has been studied by Patel et al.,[7,9,10] who measured force–distance curves of poly(2-pyridine)/polystyrene (PV2P/PS) in a good solvent (toluene at 32 °C) at various lengths of the nonadsorbing PS block. At constant length of the adsorbing PV2P block they could merge their force curves approximately into one master curve by plotting the measured force versus $D/2L_0$, where D is the distance between the two mica sheets and L_0 is

a theoretical layer thickness obtained from scaling laws for terminally anchored chains. In agreement with our results for the hydrodynamic layer thickness, it varies linearly with the length of the nonadsorbing block.

For diblock copolymers in poor solvents we find attraction at large plate separations as a result of osmotic forces, in agreement with experimental results.[7,9,10,14] The magnitude of the attraction is up to 10 times weaker than for corresponding homopolymers,[20] which agrees very well with the observations of Patel et al.[7,9,10] but not with the measurements of Marra and Hair.[14] These latter authors found for PEO/PS diblock copolymers with different block lengths the same order of magnitude of attraction as for a PS homopolymer.

Conclusions

The free energy of interaction can be calculated in a straightforward way from our previously presented self-consistent-field theory for the adsorption of block copolymers from a multicomponent mixture. We have extended the concepts of full and restricted equilibrium, as introduced by Scheutjens and Fleer for a binary mixture, toward a multicomponent mixture.

At full equilibrium, when the molecules can freely diffuse out or into the gap between the two surfaces, we found for diblock copolymers, as a rule, a repulsive interaction. Attractive interaction is only found when the surface affinities of both blocks are very close.

If the diblock copolymers cannot diffuse out of the gap when the surfaces are brought closer, i.e., in the case of restricted equilibrium, the interaction is always repulsive in good solvents. The repulsion originates from osmotic effects; for block copolymers the attractive contribution due to bridging is small or absent. In poorer solvents for the nonadsorbing block, there is an osmotic attraction at large separations. Attraction is observed as soon as χ is just above 0.5 since strongly adsorbed diblock copolymers have essentially no translational entropy so that they behave as infinitely long chains. At short distances the interaction is always repulsive because the segments are incompressible. The interaction curves for diblock copolymers are virtually the same as those for grafted chains with the same amount and length of the nonadsorbing tails, but they are shifted to slightly larger plate separations.

The interaction curves depend strongly on the chain composition. There is a direct relation between the repulsion and the adsorbed amount. For good solvents, the separation where the onset of interaction is found increases with increasing adsorbed amount and with increasing length of the nonadsorbing block. In most cases this separation corresponds to twice the hydrodynamic layer thickness. In the case of restricted equilibrium and a good solvent we have been able to scale the interaction curves of a diblock copolymer with the layer thickness, such that they merge approximately into one master curve.

For ABA triblock copolymers with adsorbing A segments and nonadsorbing B segments in a good solvent, we find attraction at large separations because of bridging. Comparison with experimental data shows, for most cases, excellent agreement.

References and Notes

(1) Vincent, B. *Adv. Colloid Interface Sci.* **1974**, *4*, 197.
(2) Tadros, T. F. In *The Effect of Polymers on Dispersion Properties*; Tadros, T. F., Ed.; Academic Press: London, 1982, p 1.
(3) Napper, D. H. *Polymeric Stabilisation of Colloidal Dispersions*; Academic Press: London, 1983.
(4) Cohen Stuart, M. A.; Cosgrove, T.; Vincent, B. *Adv. Colloid Interface Sci.* **1986**, *24*, 143.
(5) Hopkins, A.; Howard, G. J. *J. Polym. Sci., Part A-2* **1971**, *9*, 841.
(6) Dawkins, J. V.; Taylor, G. *J. Chem. Soc., Faraday Trans. 1* **1980**, *76*, 1263.
(7) Hadziioannou, G.; Patel, S.; Granick, S.; Tirrell, M. *J. Am. Chem. Soc.* **1986**, *108*, 2869.
(8) Baker, J. A.; Berg, J. C. *Langmuir* **1988**, *4*, 1055.
(9) Patel, S. S. Ph.D. Thesis, University of Minnesota, 1988.
(10) Patel, S.; Tirrell, M.; Hadziioannou, G. *Colloid Surf.* **1988**, *31*, 157.
(11) Taunton, H. J.; Toprakcioglu, C.; Klein, J. *Macromolecules* **1988**, *21*, 3333.
(12) Ansarifar, M. A.; Luckham, P. F. *Polymer* **1988**, *29*, 329.
(13) Ansarifar, M. A.; Luckham, P. F. *Polym. Commun.* **1988**, *29*, 177.
(14) Marra, J.; Hair, M. L. *Colloids Surf.* **1989**, *34*, 215.
(15) Tassin, J. F.; Siemens, R. L.; Tang, W. T.; Hadziioannou, G.; Swalen, J. D.; Smith, B. A. *J. Phys. Chem.* **1989**, *93*, 2106.
(16) Evers, O. A. Ph.D. Thesis, Wageningen University, 1990.
(17) Evers, O. A.; Scheutjens, J. M. H. M.; Fleer, G. J. *Macromolecules* **1990**, *23*, 5221.
(18) Scheutjens, J. M. H. M.; Fleer, G. J. *J. Phys. Chem.* **1979**, *83*, 1619.
(19) Scheutjens, J. M. H. M.; Fleer, G. J. *J. Phys. Chem.* **1980**, *84*, 178.
(20) Scheutjens, J. M. H. M.; Fleer, G. J. *Macromolecules* **1985**, *18*, 1882.
(21) Evers, O. A.; Scheutjens, J. M. H. M.; Fleer, G. J. *J. Chem. Soc., Faraday Trans.* **1990**, *86*, 1333.
(22) Van Lent, B. Ph.D. Thesis, Wageningen University, 1989.
(23) Van Lent, B.; Israels, R.; Scheutjens, J. M. H. M.; Fleer, G. J. *J. Colloid Interface Sci.* **1990**, *137*, 380.
(24) Whitmore, M. D.; Noolandi, J. *Macromolecules* **1990**, *23*, 3321.
(25) Scheutjens, J. M. H. M.; Fleer, G. J.; Cohen Stuart, M. A. *Colloids Surf.* **1986**, *21*, 285.
(26) Israelachvili, J. N.; Adams, G. E. *Nature (London)* **1976**, *262*, 774.
(27) Israelachvili, J. N.; Adams, G. E. *J. Chem. Soc., Faraday Trans. 1* **1978**, *74*, 975.
(28) Israelachvili, J. N. *Intermolecular and Surface Forces*; Academic Press: London, 1985.
(29) Deryagin, B. *Kolloid-Z.* **1934**, *69*, 155.
(30) de Gennes, P.-G. *Adv. Colloid Interface Sci.* **1987**, *27*, 189.